Dalton Transactions

COMMUNICATION

View Article Online
View Journal | View Issue

Cite this: *Dalton Trans.*, 2014, **43**, 2356

Received 30th September 2013,
Accepted 3rd October 2013

DOI: 10.1039/c3dt52724g

www.rsc.org/dalton

Design and self-assembly of variform organometallic macrocycle with terminal imidazole-based bridging ligands utilizing joints twist and rotation†

Tong Wu, Yue-Jian Lin and Guo-Xin Jin*

Organometallic macrocycles based on bridge ligands with terminal imidazole groups show the formation of various patterns. The end imidazolyl finishes the conjugated system on the back bone and can freely twist or rotate just like the joints of a human body such as the knee and wrist.

In recent decades, organometallic macrocycles have attracted significant attention due to their tuneable cavities/radius, shape recognition and complex interpenetration.[1] The cage with a large and suitable cavity can encapsulate different guest molecules with the aim of drug targeted delivery or fluorescence labeling.[2] Changing the size of the spacers to tune the distance between two functional groups such as ethenyl can make the photochemical [2 + 2] cycloadditions easily occur under ultraviolet irradiation.[3] It's crucial that even a slight change in the shape of their backbones can make their relevant properties convert dramatically.

Following this idea, we have designed a series of bridge ligands with a terminal imidazole group as a flexible knuckle. In this type of ligand, the imidazolyl can rid itself of backbone π-conjugate system control and rotate freely. Its rotation by a large margin also can drive the adjacent aromatic ring to revolve and twist. This kind of motion is considered as the mechanical arm behavior.[4] In this system, they need to drive upper arm swing with the help of the torsional moment from their wrists and lower arms. Based on similar theories and principles, we expect to find a flexible mode to satisfy the configuration requirements of organometallic macrocycles.

As shown in Scheme 1, two kinds of bridge ligand L_1 and L_2 were chosen as our experimental subject. First, we just made a small change to the normal linear bridge ligands, the *p*-DiImBz (*p*-diimidazolylbenzene) was employed and the

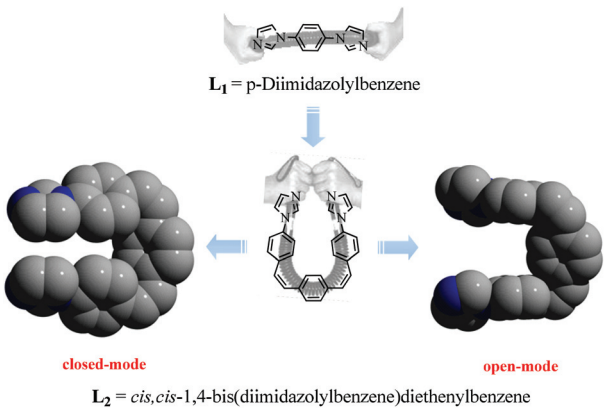

Scheme 1 Two quite different imidazole-based bridging ligands.

tetranuclear complexes that bear the BiBzIm(2,2′-bisbenzimidazole) ligand, $[Cp^*_4M_4(p\text{-DiImBz})_2(BiBzIm)_2](OTf)_4$ (**2a**: M = Ir, **2b**: M = Rh) were designed and synthesized. Then the binuclear macrocycle that bears the BiBzIm or tetraacetylethane ligand, formulated as $[Cp^*_2M_2(cis,cis\text{-}L_2)(BiBzIm)](OTf)_2$ (**3a**: M = Ir, **3b**: M = Rh) and $[Cp^*_2M_2(cis,cis\text{-}L_2)(tetraacetylethane)](OTf)_2$ (**4a**: M = Ir, **4b**: M = Rh) was prepared as orange crystals *via* **1a′** or **1b′** with four equivalents of AgOTf and subsequent reaction with *cis*,*cis*-L_2 (*cis*,*cis*-1,4-bis(diimidazolylbenzene)diethenylbenzene) in methanol at room temperature (ratio = 1 : 1) (Scheme 2).

The ^{1}H NMR spectrum of **2b** showed four singlets at δ = 1.87, 6.67, 7.60, 7.17 and 5.71 ppm in a 60 : 8 : 4 : 4 : 4 intensity ratio, due to Cp*, centra-phenyl and imidazolyl protons, respectively. In addition, the structure was determined by single crystal X-ray analysis. According to the crystal structure in Fig. 1, the cation **2b** reveals that this complex possesses a standard rhombus structure in the top view bridge by a *p*-DiImBz ligand between two spacers of BiBzIm with dimensions of 9.8777(6) × 11.8306(8) Å (S4-Fig. 2†). That's quite different from other macrocycles reported in our previous research which are mostly rectangles.[5] The key point is that

Shanghai Key Laboratory of Molecular Catalysis and Innovative Material, Department of Chemistry, Fudan University, Shanghai, 200433, P. R. China. E-mail: gxjin@fudan.edu.cn; Fax: (+86)-21-65643776

† Electronic supplementary information (ESI) available: Experimental details and crystal structure determination. CCDC 948275 (**2b**), 948276(**3a**), 948277 (**3b**), and 948278 (**4b**). For ESI and crystallographic data in CIF or other electronic format see DOI: 10.1039/c3dt52724g

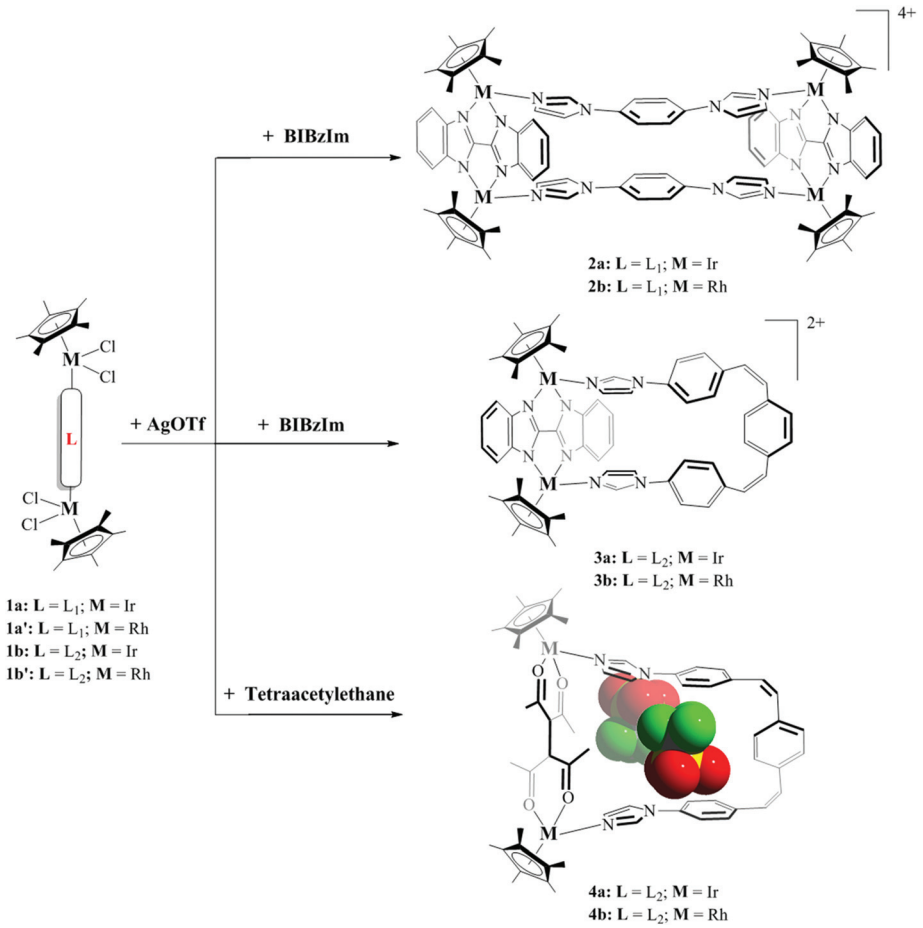

Scheme 2 Synthesis of **2a–4b** (The guest anions in **4a**, **4b** are OTf^-).

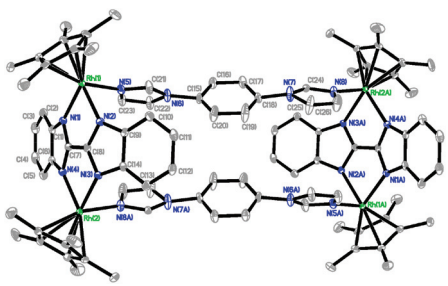

Fig. 1 Cation structure of **2b** with thermal ellipsoids drawn at the 30% level. Hydrogen atoms are omitted for clarity. Selected distances (Å) and angles (°): Rh(1)–N(1) 2.140(2), Rh(1)–N(2) 2.163(2), Rh(1)–N(5) 2.115(3), N(6)–C(15) 1.472(12), Rh(2)–N(3) 2.157(2), Rh(2)–N(4) 2.170(2), Rh(2)–N(8A) 2.121(3), N(5)–Rh(1)–N(1) 86.76(10), N(5)–Rh(1)–N(2) 85.75(10), C(21)–N(5)–Rh(1) 124.9(2), C(23)–N(5)–Rh(1) 128.5(2), N(8A)–Rh(2)–N(3) 85.48(10), N(8A)–Rh(2)–N(4) 87.99(10), C(24)–N(8)–Rh(2A) 125.1(8), C(26)–N(8)–Rh(2A) 126.8(5). The symmetry codes are A: $-x, -y + 2, -z + 1$.

the *p*-DiImBz ligands have their imidazolyl groups twisted to 60.0° and 32.3° respectively when they play the role of building blocks here. That is a dramatic trend of deformation but not revolutionary, because they are limited by the linear backbone. How about ligands with longer and folded backbones such as *cis*,*cis*-L_2?

The *cis*,*cis*-L_2, as shown in Scheme 1, has a length of about 24.0 Å which can give the terminal imidazolyl groups more room to rotate and occurs as a cooperative effect of their adjacent benzene ring due to the mechanical behavior we have mentioned. Because of this behavior, they can't self-assemble to form the tetranuclear complex but the binuclear complex instead. After two different kinds of spacers were employed to this system, **3a–b** and **4a–b** were obtained as shown in Scheme 2.

The cation in Fig. 2 reveals that complex **3b** possesses a D-shape structure in the side view bridged by *cis*,*cis*-L_2 and clamped the narrow spacer tightly. The backbone atoms N5, N7, C18, C21, C24, C25, C32, C33, C34 and C37 are located in the same plane. Based on this plane, the imidazole rings rotate 65.041° and 70.614°, the side-benzenes rings rotate 35.981° and 33.733°, the centra-benzene ring rotates 40.737°. The two side-benzene rings form an angle of 68.605°. From the space-filling cation, we know there is scarcely room for cavity and guest molecules in its arm and the distance between the inner side hydrogen atoms on the two benzene

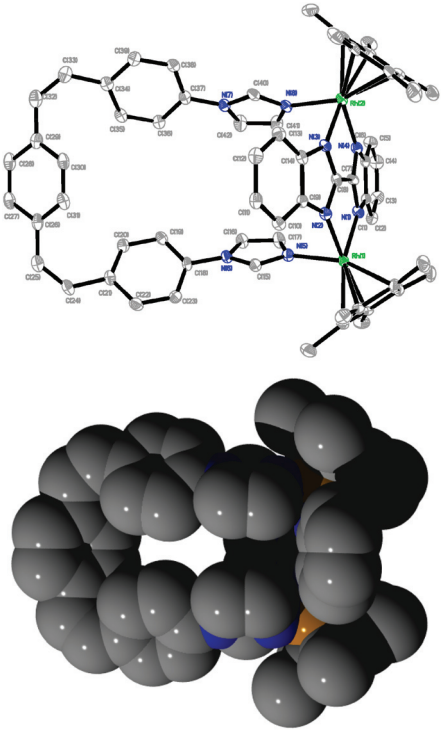

Fig. 2 Cation structure of **3b** with thermal ellipsoids drawn at the 30% level (Rh orange; N blue; C gray). Hydrogen atoms are omitted for clarity. Selected distances (Å) and angles (°): Rh(1)–N(1) 2.149(4), Rh(1)–N(2) 2.190(4), Rh(1)–N(5) 2.101(4), N(6)–C(18) 1.442(6), C(24)–C(25) 1.338(8), Rh(2)–N(3) 2.163(4), Rh(2)–N(4) 2.126(4), Rh(2)–N(8) 2.104(4), N(7)–C(37) 1.438(7), C(32)–C(33) 1.323(8), N(5)–Rh(1)–N(1) 87.29(16), N(5)–Rh(1)–N(2) 85.58(16), C(25)–C(24)–C(21) 129.2(6), C(24)–C(25)–C(26) 128.7(6), N(8)–Rh(2)–N(3) 85.81(16), N(8)–Rh(2)–N(4) 87.62(16), C(33)–C(32)–C(29) 129.0(6), C(32)–C(33)–C(34) 127.8(6). The symmetry codes are A: $-x$, $-y+2$, $-z+1$.

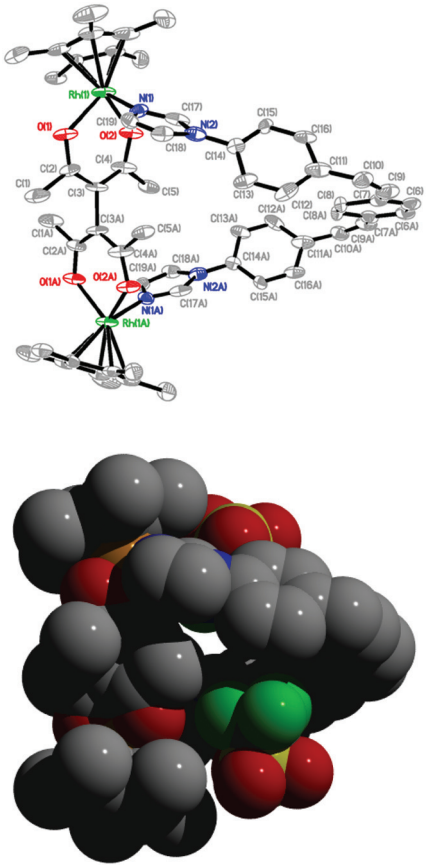

Fig. 3 Cation structure of **4b** with thermal ellipsoids drawn at the 30% level (Rh orange; N blue; C gray; O red; F green, S yellow). Hydrogen atoms are omitted for clarity. Selected distances (Å) and angles (°): Rh(1)–O(1) 2.069(8), Rh(1)–O(2) 2.065(7), Rh(1)–N(1) 2.082(8), N(2)–C(14) 1.400(13), C(9)–C(10) 1.299(17), O(1)–C(2) 1.267(10), O(2)–C(4) 1.270(9), O(1)–Rh(1)–N(1) 84.0(3), O(2)–Rh(1)–N(1) 86.1(3), O(2)–Rh(1)–O(1) 88.7(3), C(9)–C(10)–C(11) 128.2(11), C(10)–C(9)–C(7) 131.2(12), C(17)–N(1)–Rh(1) 125.3(7), C(19)–N(1)–Rh(1) 131.1(8). The symmetry codes are A: $-x+1/2$, $-y+3/2$, z.

rings is 2.7189(2) Å, a very strong hydrogen bond intramolecular interaction. This status is called closed-mode.

The cation in Fig. 3 shows that complex **4b** possesses a spiral D-shape in the stereoscopic view with two OTf anions in its cavity. The cation lies about a two fold axis. The backbone atoms C(6), C(7), C(8), C(9), C(6A), C(7A), C(8A) and C(9A) are located in the same plane. Based on this plane, the olefin bonds twist for 14.965°, the side-benzene rings rotate 66.130°, the imidazole rings rotate 34.033°. The two side-benzene rings form an angle of 7.416° nearly parallel to each other which like two doors open to encapsulate the anion guest from two sides which is called open-mode as shown in the space-filling cation of Fig. 3. In the ^{19}F NMR spectrum, complex **3b** has only one signal at −78.19 ppm (free OTf^-). But the complex **4b** shows three signals: −78.19 (free OTf^-), −77.89 and −78.74 (OTf^- encapsulated) ppm as evidence of structural stability in solution.

Compared with the cation **3b**, the distance of the two rhodium atoms are stretched from 5.5895(7) Å to 8.2353(14) Å and the shape of the spacer is more like a pillar rather than a narrow fence. This ligand also can rotate itself to satisfy the angle of coordination site. That is why it can prop the two imidazole rings open and make the *cis*,*cis*-L_2 distorted as part of a spring. The two planes passed by two diacetylethane groups are crossed at an angle of 87.265°.

Here the complex **4b** encapsulates two OTf anions in the cavity. Different to other aromatic guests, there is no π···π stacking interaction to make them insert into the cavity, but there are more than six hydrogen bonds around each anion (two of them come from cp* for 2.6274(118) and 2.6570(154) Å, one comes from the imidazole ring for 2.8589(138) Å, three of them come from the centra-benzene ring for 2.9334(120), 3.3330(173) and 2.4107(114) Å and the last one comes from the methyl group of the tetraacetylethane ligand for 2.5322(189) Å as shown in ESI-S4-Fig. 4†).[6] Two factors cooperate with each other to form this host–guest system: the long spacer lets the benzene rings rotate followed by the imidazole rings to form an open-mode cavity like an open door; hydrogen bonds between the cp* fragments and hydrogen atoms with the guest molecules catch the anions tightly.

In summary, we have described a type of bridge ligand with terminal imidazolyl groups as building blocks of organometallic macrocycles, which occurs through mechanical arm behaviour to control the self-assembly for closed-mode or open-mode structures with the help of different spacers. The shape of the open-mode complex looks like a double-faced bowl which encapsulated the two anions embedded in each side, respectively. This system provides us with a new concept to build various structures to enhance the corresponding properties.

Experimental section

All manipulations were performed under an atmosphere of nitrogen using standard Schlenk techniques. Solvents were dried and deoxygenated by MBraun Solvent Purification System and collected just before use. $[Cp^*MCl_2]_2$(M = Ir/Rh)[7a] tetraacetylethane[7b] and 2,2′-bisbenzimidazole[7c] were prepared according to literature methods. The *cis*,*cis*-L_2 was prepared as described in ESI S1.†[6] IR spectra were recorded on a Nicolet AVATAR-360 IR spectrometer, elemental analyses were carried out on an Elementar III Vario EI Analyzer. ^{1}H-NMR spectra were obtained on a Bruker DMX-500 or a Bruker DMX-400 spectrometer in DMSO-d_6 solution.

Synthesis of **2a**, **2b**: to a solution of $[Cp^*MCl(\mu\text{-}Cl)]_2$(M = Ir/Rh) (40.0 mg/30.0 mg, 0.05 mmol) in dry CH_3OH (10 mL) was added *p*-DiImBz (10.5 mg, 0.05 mmol) at room temperature. After vigorous stirring for about 4 h, AgOTf (51.2 mg, 0.20 mmol) was added to the solution for 5 h. Finally, 2,2′-bisbenzimidazole (11.7 mg, 0.05 mmol) was added into the solution with vigorous stirring for 5 h. After the reaction was completed, the solution was filtered to remove undissolved compounds. The pure products were obtained by recrystallization through the diffusion of ether into the filtrate, giving the crystals of **2a** (light yellow, 46.44 mg, 65%) and **2b** (bright orange, 44.34 mg, 71%).

Synthesis of **3a**, **3b**, **4a** and **4b**: $[Cp^*MCl(\mu\text{-}Cl)]_2$(M = Ir/Rh) (20.0 mg/15.0 mg, 0.025 mmol) was dissolved in dry CH_3OH (10 mL) then *cis*,*cis*-L_2 (10.4 mg, 0.025 mmol) was added at room temperature. After vigorous stirring for about 4 h, AgOTf (25.6 mg, 0.10 mmol) was added to a suspension for 5 h, followed by adding 2,2′-bisbenzimidazole (5.85 mg, 0.025 mmol)/tetraacetylethane (5.0 mg, 0.025 mmol) into the solution and vigorous stirring for 5 h. After the reaction was complete, the solution was filtered to remove undissolved compounds. The pure products were obtained by recrystallization through diffusion of ether into the filtrate, giving the crystals of **3a** (yellow, 34.74 mg, 83%), **3b** (orange, 33.27 mg, 89%), **4a** (yellow, 27.2 mg, 68%) and **4a** (orange, 26.99 mg, 76%).

The characterization data of complex **2a–4b** are shown in ESI-Table 1.†[6]

All single crystals were immersed in the mother liquor and sealed in thin-walled glass. Data were collected on a CCD-Bruker SMART APEX system. All the determinations of unit cell and intensity data were performed with graphite-monochromated Mo Kα radiation (λ = 0.71073 Å). All the data were collected at room temperature using the ω scan technique. These structures were solved by direct methods, using Fourier techniques, and refined on F^2 by a full-matrix least-squares method. All the calculations were carried out with the SHELXTL program.[8]

2b: in asymmetric unit of this data, the diimidazole ligand was disordered and it was divided into two parts (60 : 40 for the benzene ring and 52 : 48 for imidazole ring). 4 ISOR, 2 DFIX and 1 FLAT instructions were used to restrain the ligand so that there were 28 restraints in the data.

3a: in asymmetric unit of **3a**, there were disordered solvents (three diethyl ether and four methanol molecules) which could not be restrained properly. Therefore, the SQUEEZE algorithm was used to omit them. One triflate anion was disordered and it was divided into two parts (48 : 52). O4, O6, O4′ and O6′ were refined isotropically because of NPD and other non-hydrogen atoms were refined isotropically. 5 ISOR and 12 DFIX instructions were used so that there were 42 restraints in the data.[9]

3b: in asymmetric unit of **3b**, there were disordered solvents (three diethyl ether and four methanol molecules) which could not be restrained properly. Therefore, the SQUEEZE algorithm was used to omit them. C64, C66 and C68 were refined isotropically because of NPD and other non-hydrogen atoms were refined anisotropically. Two ISOR and four DFIX instructions were used to restrain the anions and solvents so that there were 16 restraints in the data.

4b: in the asymmetric unit of this data, there was a disordered water molecule which could not be restrained properly. Therefore, the SQUEEZE algorithm was used to omit it. 9 DFIX, 4 ISOR and 1 DELU instructions were used to restrain the Cp* fragment and triflate anion so that there were 35 restraints in the data.

Acknowledgements

This work was supported by the National Science Foundation of China (91122017, 21374019), the Program for Changjiang Scholars and Innovative Research Team in University (IRT1117) and the Shanghai Science and Technology Committee (13JC1400600, 13DZ2275200).

Notes and references

1 For example, see: (*a*) H. Amouri, C. Desmarets and J. Moussa, *Chem. Rev.*, 2012, **112**, 2015–2041; (*b*) J.-S. Chen, G.-J. Zhao, T. R. Cook, K.-L. Han and P. J. Stang, *J. Am. Chem. Soc.*, 2013, **135**, 6694–6702; (*c*) S. Mirtschin, A. Slabon-Turski, R. Scopelliti, A. H. Velders and K. Severin, *J. Am. Chem. Soc.*, 2010, **132**, 14004–14005; (*d*) B. Kilbas, S. Mirtschin, R. Scopellitia and K. Severin, *Chem. Sci.*, 2012, **3**, 701–704; (*e*) S.-L. Huang, Y.-J. Lin, T. S. Andy Hor and G.-X. Jin, *J. Am. Chem. Soc.*, 2013, **135**, 8125–8128; (*f*) S.-J. Li, J.-Y. Huang, T. R. Cook, J. B. Pollock, H. Kim, K.-W. Chi and

P. J. Stang, *J. Am. Chem. Soc.*, 2013, **135**, 2084–2087; (*g*) V. Vajpayee, Y. H. Song, T. R. Cook, H. Kim, Y. Lee, P. J. Stang and K.-W. Chi, *J. Am. Chem. Soc.*, 2011, **133**, 19646–19649; (*h*) Y. Yamauchi, Y. Hanaoka, M. Yoshizawa, M. Akita, T. Ichikawa, M. Yoshio, T. Kato and M. Fujita, *J. Am. Chem. Soc.*, 2010, **132**, 9555–9557; (*i*) M. Fujita, *Acc. Chem. Res.*, 1999, **32**, 53–61; (*j*) Y.-F. Han, G.-X. Jin and F. E. Hahn, *J. Am. Chem. Soc.*, 2013, **135**, 9263.

2 (*a*) M. Fujita, M. Tominaga, A. Hori and B. Therrien, *Acc. Chem. Res.*, 2005, **38**, 369–378; (*b*) B. Therrien, G. Süss-Fink, P. Govindaswamy, A. K. Renfrew and P. J. Dyson, *Angew. Chem., Int. Ed.*, 2008, **47**, 3773–3776; (*c*) F. Schmitt, J. Freudenreich, N. P. E. Barry, L. Juillerat-Jeanneret, G. Süss-Fink and B. Therrien, *J. Am. Chem. Soc.*, 2012, **134**, 754; (*d*) Y. Yamaguchi, M. Yoshizawa, M. Akita and M. Fujita, *J. Am. Chem. Soc.*, 2010, **132**, 960–966; (*e*) Y.-F. Han, H. Li and G.-X. Jin, *Chem. Commun.*, 2010, **46**, 6879–6890; (*f*) T. Wu, Y.-J. Lin and G.-X. Jin, *RSC Adv.*, 2013, **3**, 11476–11479.

3 (*a*) G. M. J. Schmidt, *Pure Appl. Chem.*, 1971, **27**, 647–678; (*b*) L. R. MacGillivray, G. S. Papaefstathiou, T. Frišćić, T. D. Hamilton, D.-K. Bučar, Q. Chu, D. B. Varshney and I. G. Georgiev, *Acc. Chem. Res.*, 2008, **41**, 280–291; (*c*) M. H. Mir, J. X. Ong, G. K. Kole, G. K. Tan, M. J. McGlinchey, Y. Wu and J. J. Vittal, *Chem. Commun.*, 2011, **47**, 11633–11635; (*d*) Q. Chu, D. C. Swenson and L. R. MacGillivray, *Angew. Chem., Int. Ed.*, 2005, **44**, 3569–3572; (*e*) T. Wu, L.-H. Weng and G.-X. Jin, *Chem. Commun.*, 2012, **48**, 4435–4437; (*f*) Y.-F. Han, Y.-J. Lin, W.-G. Jia, G.-L. Wang and G.-X. Jin, *Chem. Commun.*, 2008, 1807–1809; (*g*) W.-B. Yu, Y.-F. Han, Y.-J. Lin and G.-X. Jin, *Chem.–Eur. J.*, 2011, **17**, 1863–1871.

4 (*a*) E. R. Kay, D. A. Leigh and F. Zerbetto, *Angew. Chem., Int. Ed.*, 2007, **46**, 72–191; (*b*) N. Koumura, R. W. J. Zijlstra, R. A. van Delden and B. L. Feringa, *Nature*, 1999, **401**, 152–155; (*c*) B. L. Feringa, *Acc. Chem. Res.*, 2001, **34**, 504–513; (*d*) G. Vives, A. Carella and J. P. Launay, *Coord. Chem. Rev.*, 2008, **252**, 1451–1459.

5 (*a*) Y. F. Han, W. G. Jia, W. B. Yu and G. X. Jin, *Chem. Soc. Rev.*, 2009, **38**, 3419; (*b*) T. Wu, Y.-J. Lin and G.-X. Jin, *Dalton Trans.*, 2013, **42**, 82–88; (*c*) Y.-F. Han, W.-G. Jia, Y.-J. Lin and G.-X. Jin, *Angew. Chem., Int. Ed.*, 2009, **48**, 6234–6238.

6 See ESI.†

7 (*a*) C. White, A. Yates and P. M. Maitles, *Inorg. Synth.*, 1992, **29**, 228–230; (*b*) J. Z. Vlahakis, S. Mitu, G. Roman, E. P. Rodriguez, I. E. Crandall and W. A. Szarek, *Bioorg. Med. Chem.*, 2011, **19**, 6525–6542; (*c*) M. C. ReZende, C. A. Marques, E. L. Dall'Oglio and C. Zucco, *Liebigs Ann.*, 1997, **397**, 925–929.

8 G. M. Sheldrick, *SHELXL-97*, Universität Göttingen, Germany, 1997.

9 A. L. Spek, *Acta Crystallogr., Sect. D: Biol. Crystallogr.*, 2009, **65**, 148–155.

